nature communications

Article

https://doi.org/10.1038/s41467-025-61857-0

Bioinspired transfer methylation enabled by a photoactive reagent

Received: 10 April 2025

Accepted: 3 July 2025

Published online: 18 September 2025

Check for updates

Ding Zhang[1,2,6], Weiqiu Liang[3,6], Zhihan Zhang[4,6] ✉, Lida Tan[5], Zehao Yuan[1,2], Zhennan Hu[1,2], Zhibo Liu[3] ✉, Chao-Jun Li[5] ✉ & Jianbin Li[1,2] ✉

Radical methylation ranks among the most important yet challenging transformations in chemistry and biology, which often involves small and unstable radical intermediates, such as the methyl radical, and results in low reactivity and poor selectivity. Herein, we report a photoactive, biomimetic reagent to address some facets of these challenges by leveraging a bulky and stabilised α-aminomethyl radical, which can offer enhanced control over radical generation and transfer. Our bioinspired transfer methylation protocol enables direct and selective C(sp^2)–H methylation across a wide spectrum of heteroarenes, from simple scaffolds to complex drug molecules, including the thus far elusive C4-methylation of free quinolines. Mechanistic studies reveal that the unique α-aminomethyl radical intermediate undergoes an addition-elimination sequence reminiscent of natural methyltransferases and yields balanced reactivity and selectivity.

Radical methylation has long challenged chemists due to the involvement of difficult-to-control intermediates like methyl radicals[1–4]. In contrast, nature manages such a transformation with unparalleled efficiency. For example, the recently characterised radical *S*-adenosyl-L-methionine-dependent methyltransferase (rSAM MT) TbtI exemplifies this by regioselectively methylating a single thiazole among six in the complex hexazole core of Thiomuracin A1, which was enabled by a bulky SAM-derived methyl radical (Fig. 1A)[5,6]. However, replicating such a biosynthetic capability with superior reactivity and selectivity, particularly for the late-stage methylation of complex molecules, remains challenging in laboratory settings due to the scarcity of suitable chemical tools.

Encouraged by the elegant paradigm of rSAM MT and given the centrality of heteroarenes in many biological processes[7] and medicinal campaigns[8,9], chemists are striving to expand their chemical repertoire to perform heteroaromatic methylation under radical manifolds (Fig. 1B)[1,10]. Among these efforts, seminal work by Minisci and others in the 1970s demonstrated the feasibility of radical methylation of a few heteroaromatic compounds, albeit under relatively harsh thermal conditions involving strong acids and excessive peroxides to generate the methyl radical[11]. The non-selective monomethylation and dimethylation of quinoline (**1b** + **1b'** vs **2b**), as well as the virtually equimolar C2- and C4-methylation products (**1b** vs **1b'**), emphasise the difficulty in taming methyl radical under abiotic conditions. In advancing the radical methylation under milder conditions, MacMillan's group and one of us made a breakthrough towards the room-temperature methylation of heteroarenes with hydroxymethyl radical, which was generated from methanol by the dual photoredox catalysis[12] and photoexcited azines[13], respectively. Not long after, Zuo and his co-workers took advantage of alkoxy radical-mediated[14,15] hydrogen atom transfer (HAT)[16] and strategised the cross-dehydrogenative coupling (CDC) between methane and isoquinoline via methyl radical[17–20].

Despite these advances, the inherent instabilities of the requisite (hydroxy)methyl radicals[21–23] usually mandate the use of largely

[1]School of Science and Engineering, The Chinese University of Hong Kong, Shenzhen, Guangdong, China. [2]Guangdong Basic Research Centre of Excellence for Aggregate Science, School of Science and Engineering, The Chinese University of Hong Kong, Shenzhen, Guangdong, China. [3]Beijing National Laboratory for Molecular Sciences, Radiochemistry and Radiation Chemistry Key Laboratory of Fundamental Science, Key Laboratory of Bioorganic Chemistry and Molecular Engineering of Ministry of Education, College of Chemistry and Molecular Engineering, Peking University, Beijing, China. [4]College of Chemistry, Central China Normal University, Wuhan, Hubei, China. [5]Department of Chemistry, FRQNT Centre for Green Chemistry and Catalysis, McGill University, Montreal, Quebec, Canada. [6]These authors contributed equally: Ding Zhang, Weiqiu Liang, Zhihan Zhang. ✉e-mail: zhihanzhang@ccnu.edu.cn; zbliu@pku.edu.cn; cj.li@mcgill.ca; jianbinli@cuhk.edu.cn

https://doi.org/10.1038/s41467-025-61857-0

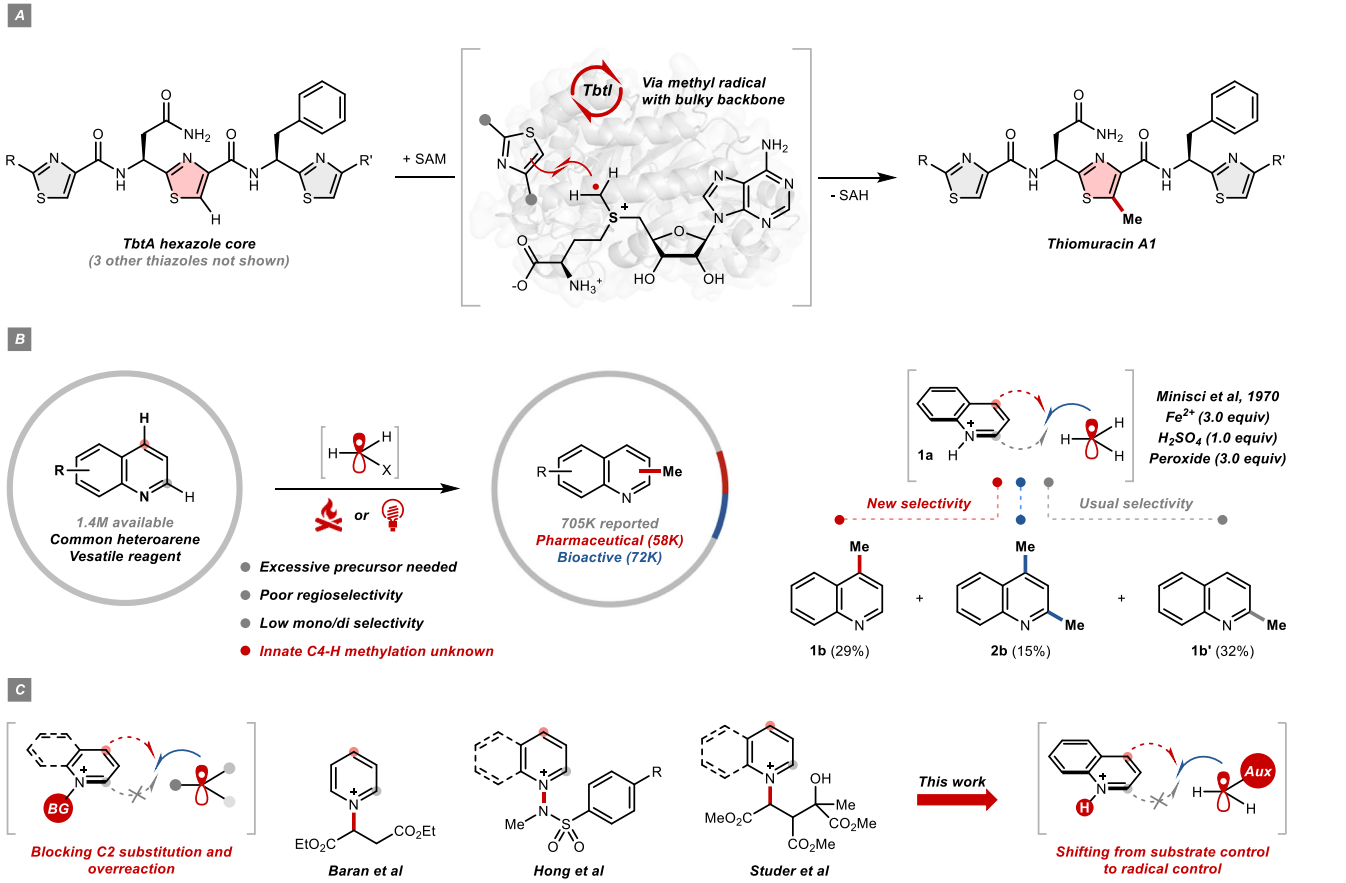

Fig. 1 | Introduction. A Radical methylation in nature by TbtI. rSAM, radical *S*-adenosyl-L-methionine methyltransferase. SAH, *S*-adenosyl-L-homocysteine. **B** Radical methylation via methyl radical and its equivalents. **C** Representative protecting group strategies for radical C4-functionalization of azines. BG, blocking group. Aux, auxiliary group.

excessive precursors (e.g., solvent-level quantities of methanol[12,13,24] and pressurised methane[17,25,26]) or reactive reagents (e.g., peroxide[11,27–29]) to enforce their generation[30]. As such, these radical systems could be unmanageable, resulting in overalkylation and other off-target reactivities[12,13]. Moreover, similar to Minisci's earlier findings, regioselectivity was poor for unbiased heteroarene substrates, which manifested most visibly in C2- and C4-unsubstituted quinolines. For protonated **1a**, Fukui indices imply minimal differentiation at C2 (f = 0.13) and C4 (f = 0.13); yet, slight bias at C2 is frequently observed in practice. Consequently, a nearly inseparable mixture of unconsumed starting material (**1a**), monomethylation (**1b** and **1b'**) and dimethylation (**2b**) products would ensue because of the small size and electron neutrality of the methyl group. Similar issues also persist in other radical C(sp^2)–H functionalisations of free quinolines and pyridines[31], which were partially resolved by leveraging the *N*-blocking groups to minimise C2-substitution and overreaction (Fig. 1C)[32–37]. However, to the best of our knowledge, the innate radical C4–methylation of simple quinolines remains unknown[38].

In this context, we attributed the unsatisfactory regiochemical outcome to the small size and planar geometry of (hydroxy)methyl radicals, coupled with their strong nucleophilicities (nucleophilic indices, ω^- = 0.37 and 0.49, respectively). Inspired by the rSAM MT, we sought to address these challenges by employing an enzyme-like, bulkier and more stabilised analogue of the (hydroxy)methyl radical. Following this logic, α-aminomethyl radicals derived from the readily available methylamines stand out, considering that their *N*-substituents could endow reagents with more dimensional flexibility and chemical possibilities (Fig. 2A). Hence, it is hypothesised that the *N*-Me compounds (**Ra**) could be serviceable, with their conjugated heteroaromatic backbone (auxiliary) fulfilling several purposes. Firstly, they can serve as internal photooxidants and confine the electron transfer unimolecularly, thus avoiding the need for discrete photocatalysts and redox agents to aid the radical generation[39,40]. Secondly, the stability of nascent α-aminomethyl radicals (**Rc**) will be enhanced with their nucleophilicity attenuated (ω^- = 0.36), which could further facilitate the radical generation at the cost of fewer reagents and offer more control over the radical addition. Thirdly, molecular recognition (e.g., hydrogen bonding) could pre-associate the reagent and the substrates (**Rd**), further accelerating the progress of the overall reaction. More importantly, such a non-covalent interaction could potentially biomimic the enzyme-substrate assembly that governs regioselectivity, and the steric bulk of **Rc** can limit the installation of methyl groups when multiple sites of the substrate are available to intercept radicals.

En route to such a privileged scaffold, we developed a dihydropyrimidoquinolinone (DHPQ) reagent in our prior research on radical alkylation, which can release the alkyl radical upon direct excitation[41,42] via a nitrogen radical cation intermediate (**Rb**)[43]. On this basis, we reason that by introducing poor leaving groups to suppress the β-scission, the edited DHPQ reagents could be repurposed to form α-aminomethyl radicals (**Rc**)[44,45]. Ideally, theoretical calculations unveiled that the spin density of **Rc** is mainly situated on the *N*-methylene site and delocalised over the DHPQ shield, thus being enzymologically analogous to the SAM-derived radical. As detailed below, we successfully prepared a purpose-tailored methylating reagent (**R1**) and developed its methylation methodology with broad utility. Of equal importance, we elucidated the unique reactivity and

https://doi.org/10.1038/s41467-025-61857-0

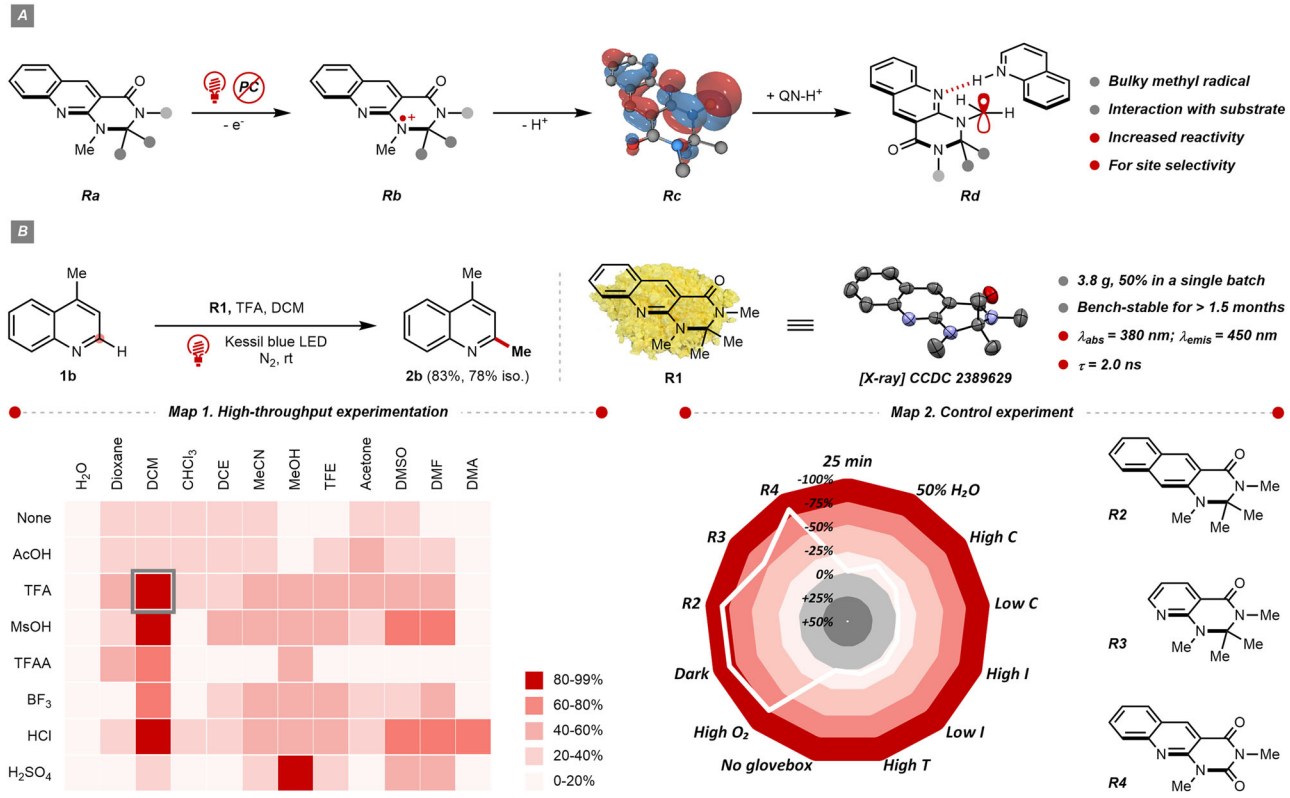

Fig. 2 | Our design and reaction discovery. A Our design of methylating reagent. Nucleophilicity index, ω⁻, in eV is computed by B3LYP/6-311 + g(d,p). QN-H⁺, quinolinium. **B** Reaction development. See the Supplementary Information for detailed conditions. General conditions: heteroarene (1.0 equiv), **R1** (1.5 equiv), 12 h. Unless otherwise specified, the yield refers to the calibrated yields using gas chromatography (GC) or nuclear magnetic resonance (NMR) spectroscopy with internal standards. Iso., isolation. Abs, absorption. Emis, emission. LED, light-emitting diode. AcOH, acetic acid. TFA, trifluoroacetic acid. MsOH, methanesulfonic acid. TFAA, trifluoroacetic acid anhydride. DCM, dichloromethane. DCE, 1,2-dichloroethane. TFE, 2,2,2-trifluoroethanol. DMSO, dimethylsulfoxide. DMF, *N*,*N*-dimethylformamide. DMA, *N*,*N*-dimethylacetamide. Low/high C, low/high concentration (0.10/0.025 M). Low/high I, low/high light intensity (23/100 W). High T, high reaction temperature (~60 °C).

selectivity of **R1** by combinatorial efforts in experimentation and computation, which uncovered a stepwise methylation pathway akin to the naturally occurring rSAM MT.

Results

Proof of concept

To entertain our hypothesis, multigram-scale synthesis of **R1** was quickly accomplished in a single batch from commodity chemicals (See Supplementary Information, Section 2.1), affording the bench-stable yellow crystalline powder to probe its photophysical properties and photochemical reactivities (Fig. 2B). In line with our simulation (Supplementary Fig. S12), the ultraviolet-visible (UV-vis) and fluorescence spectra of **R1** displayed prominent absorption (λ_{max} = 380 nm) and emission (λ_{max} = 450 nm) residing in the violet and blue regions, respectively (Supplementary Figs. S5 and S6). Besides, lifetime measurement by time-correlated single-photon counting (TCSPC) uncovered a long-lived excited state of **R1** (τ_f = 2.0 ns) (Supplementary Fig. S7).

To establish the proof of concept, **R1** was first examined with lepidine (**1b**). To accelerate the discovery of "hit" conditions, solvent and acid, two key parameters in classic Minisci-type chemistry, were systematically surveyed using our customised high-throughput screening (HTS) platform under blue light-emitting diodes (LED) irradiation (λ_{max} = 420 nm), which rapidly identified dichloromethane (DCM) and trifluoroacetic acid (TFA) as optima (Fig. 2B, Map 1). Guided by this result, the reaction conditions were further fine-tuned so that slightly excessive **R1** led to a 78% yield of isolated 2,4-dimethylquinoline (**2b**). Of note was the significantly shortened reaction time compared to other known methods (typically around 24 h), as an uncompromised yield of **2b** could be obtained within 25 min. Moreover, up to 50% water could be tolerated, laying the foundation for applying **R1** in modifying water-soluble pharmaceuticals and biomolecules. The **R1** variants (**R2**–**R4**) were less productive, indicating the importance of quinoline and *gem*-dimethyl moieties in ensuring the desired methylative reactivities. Control experiments revealed that the productivity of **R1** is insensitive to the changes in concentrations, light intensity and temperature; however, the light and inert atmosphere are indispensable (Fig. 2B, Map 2)[46].

Direct C(sp^2)–H methylation of simple *N*-heteroarenes

Next, the generality of our heteroaromatic C(sp^2)–H methylation was explored. To assess the positional selectivity of **R1**, a few representative quinolines with C2 and C4 being non-substituted were tested. With the simplest quinoline (**1a**), **R1** can provide the on-demand C4−methylation product with 5:1 regioselectivity (**1b**:**1b'**) and without detectable dimethylation product (**2b**), which remained unreported in previous literature (Fig. 3i). After intensive optimisation (See Supplementary Information, Section 2.4), we eventually found that adding water and lowering the temperature were beneficial, increasing the regioisomeric ratio to >11:1. **R1** can also methylate other quinolines that might face the C2/C4 selectivity issue and produce the desired C4-methylated products in good selectivity (**3b**, **5b** to **8b**), except for the one bearing a hindered C5-Me group (**4b**).

For comparison, two state-of-the-art MeOH-based photochemical methylation approaches were selected. Complementarily, the photocatalytic method (**M1**) showed inverted positional selectivity and

https://doi.org/10.1038/s41467-025-61857-0

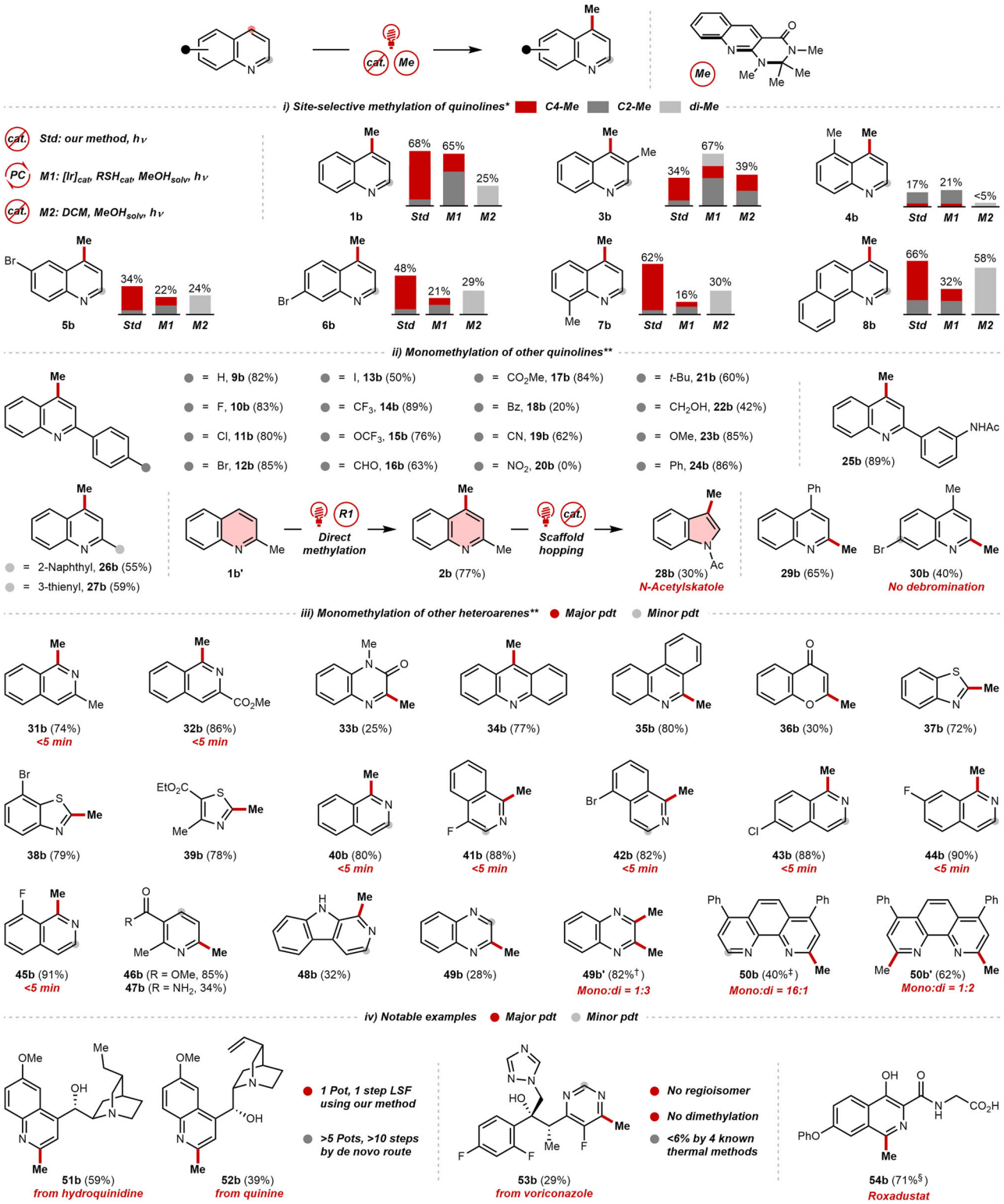

Fig. 3 | Substrate scope of C(sp^2)-methylation with heteroarenes. See the Supplementary Information for detailed conditions. General conditions: heteroarene (1.0 equiv), **R1** (1.5 equiv), TFA (3.0 equiv), DCM (0.050 M), Kessil lamp (427 nm). Potential reactive sites are highlighted in red or grey spots. Regioselectivity is determined by gas chromatography (GC) or nuclear magnetic resonance (NMR) spectroscopy. *Only the C4-methylation product is shown. C2- and C2, C4-bismethylated products are omitted for clarity. **Unless otherwise specified, monomethylation dominates (mono:di > 20:1) with high regioselectivity (no regioisomer or > 20:1 regioselectivity), and the percent yield refers to the combined products. †Heteroarene (1.0 equiv), **R1** (3.0 equiv). ‡Heteroarene (2.0 equiv), **R1** (1.0 equiv). §Total yield of methylation and amidation. Cat, catalyst. Solv, solvent. *hν*, photon. Ac, acetyl group. Pdt, product. LSF, late-stage functionalisation. TFA, trifluoroacetic acid. DCM, dichloromethane.

persistently favoured the C2-methylated products (**1b'**, **3b'** to **8b'**), like other Minisci alkylation reactions. In contrast, non-productive substrate decomposition was frequently seen with the energy-intensive UV-mediated methods (**M2**), and dimethylation was observed in most cases.

Then, the chemical versatility of **R1** on other C2- or C4-functionalised quinolines was examined (Fig. 3ii). 2-Arylquinolines with diverse functional groups underwent the site-selective C4-methylation in good to excellent yields (**9b** to **27b**). A series of electron-withdrawing functionalities, including halogen (**10b** to **13b**), trifluoromethyl (**14b**), trifluoromethoxy (**15b**), carbonyl (**16b** to **18b**), and nitrile (**19b**) groups, were tolerated. However, the 2-arylquinoline with *para*-nitro group failed to give any product, possibly due to its photodecomposition (**20b**)[47–49]. The action of **R1** on 2-arylquinolines bearing electron-donating alkyl (**21b** and **22b**) and ethereal (**23b**) as well as the neutral phenyl groups (**24b**) at *para*-positions of the 2-phenyl groups also proceeded well, and so did the one with a *meta*-amido group (**25b**). Similarly, 2-naphthyl, 2-thiophenyl and 2-methylquinolines were all effective substrates with **R1** (**26b**, **27b** and **2b**). To elaborate on the structural diversity of our scope, the quinoline methylation product **2b** was further subjected to scaffold hopping under Levin's reported conditions[50,51], accomplishing a formal C3-methylation of indole via a sequential single-carbon peripheral and skeletal editing (**28b**). In addition, methylation of C4-substituted quinolines efficiently provided the desired C2–methylated product (**29b** and **30b**). Noticeably, the UV-labile bromo group in **30b** was untouched in our case[13].

Besides quinolines, numerous heteroaromatic pharmacophores were evaluated (Fig. 3iii). Isoquinolines (**31b** and **32b**), quinoxalinone (**33b**) and more conjugated substrates, including acridine (**34b**) and phenanthridine (**35b**), were methylated efficiently. Notably, methylation with isoquinolines could be completed within 5 min, which was pronouncedly faster than other known radical methylation methods (6 to 48 hours)[12,13,22,24]. In addition to *N*-heterocycles, *O*-heteroarene like chromenone (**36b**) and five-membered *S*-heteroarenes like benzothiazoles (**37b** and **38b**) and thiazole (**39b**), which represented underexplored methylation substrates[13], were all accommodated.

Regarding heteroarenes with additional methylation sites, non-selective monomethylation and dimethylation will ensue with methods that rely on overstoichiometric methylating reagents. By comparison, our approach with a controllable substate/reagent ratio demonstrated exceptional site selectivity and minimal tendency towards overmethylation. The regioselectivity and monomethylation/dimethylation product ratio is generally over 20:1. Isoquinolines (**40b** to **45b**), pyridines (**46b** and **47b**), pyridoindole (**48b**), quinoxaline (**49b**) and phenanthroline (**50b**) all afforded the monoselective products exclusively. Dimethylation products could also be obtained, however, under forcing conditions with more reagents and prolonged time (**49b'** and **50b'**).

Late-stage C(sp^2)–H methylation of complex *N*-heteroarenes

Contrasting the maturation of higher-order alkylations, existing methylation strategies were scarcely utilised in complex molecular architectures[10,28,29]. To fill this gap, some pharmaceutically important leads and drug candidates were selected for our methylation protocol (Fig. 3iv). Quinine and hydroquinidine were methylated successfully (**51b** and **52b**), while their routine methylation processes dictate either MeLi or de novo synthesis with >10-step longest linear sequence (LLS) and Me_4Sn[52]. Methylation of voriconazole, which is reluctant under thermal conditions, also proceeded site-selectively (**53b**). Structurally and functionally complex isoquinoline could also be methylated, providing a shortened route to access the anti-anaemia medication, rosadustat (**54b**).

Mechanistic experiments

After demonstrating the synthetic merits of **R1**, we commenced mechanistic studies to rationalise its reactivity and selectivity. To begin, deuterium labelling experiments were performed to ascertain the hydrogen source of the transferred methyl group. It was found that the *N*-deuteromethylated **R5** can transfer its CD_3 group to **35a** with around 1/3 D content loss, while the *C*-deuteromethylated **R6** gave no incorporation of deuterium in **35b** (Fig. 4A, entries 1 and 2). Consistently, **R7** without any *N*-Me groups failed to afford any methylation product (Fig. 4A, entry 3). Furthermore, reactions with **R1** in the presence of CF_3CO_2D or CD_2Cl_2 partially deuterated **35b** (Fig. 4A, entries 4 and 5). Taken together, these results confirmed that the *N*-Me groups of **R1**, TFA and DCM all contributed to the product's methyl group ($n_{total} \approx 3$), thus matching the biocatalytic mode with rSAM MT. Careful analysis of **R5'** and **R6'** agreed with our initial hypothesis that demethylation occurred on the N_{amine} instead of the N_{amide} site since the former was directly involved in the photoexcitation of **R1** to engender the nitrogen radical cation (**Rb**)[43]. As expected, these demethylated byproducts were unreactive towards heteroaromatic methylation, yet they could be recycled, methylated and reused for another round of transfer methylation.

The kinetic isotope effect (KIE) was measured by the initial rate assessment with deuterated methylating reagent (**R5**) and substrate (**40a-d_1**) separately (Fig. 4B). Parallel competition between **R1** and **R5** revealed a KIE ($k_H/k_D = 1.7$), which suggested the α-N_{amine} C(sp^3)–H bond of **R1** cleavage was at least partly involved in the rate-determining step (RDS). By contrast, the KIE was insignificant ($k_H/k_D = 1.1$) in the case of α-deuterated isoquinoline (**40a-d_1**). The marginal secondary KIE indicated that the scission of the C(sp^2)–H bond of **40a** is unlikely to be rate-limiting[53], which deviated from the typical observation in Minisci-type reactions[24,54–56].

With the informative KIE in mind, we aimed to evidence the involvement of α-aminomethyl radical (**Rc**) (Fig. 4C). When subjecting hydroquinidine to our transfer methylation conditions, apart from the anticipated methylated hydroquinidine (**51b**), an aminomethylated side product (**51b'**) was isolated, which structurally resembles the flavin-containing intermediate during the nucleotide methylation catalysed by the bacterial thymidylate synthase ThyX[57]. Crucially, **51b'** can slowly photo-release the methylation product (**51b**) after detachment of the DHPQ auxiliary, thus fully agreeing with our proposed biomimetic addition and elimination mechanism with **Rc**. It is worth mentioning that a similar DHPQ-CH_2-heteroarene intermediate was also detected during the real-time monitoring of the methylation of lepidine (**1b**), although the isolation was unsuccessful (Supplementary Fig. S14). Electron-deficient olefin can trap **Rc** as well, resulting in linear and cyclised Giese-type products in an almost equal ratio (**55b** and **55b'**). To gain more direct evidence, the open-shell **Rc** was characterised by operando electron paramagnetic resonance (EPR) spectroscopy as a spin-trapping adduct with 5,5-dimethyl-1-pyrroline *N*-oxide (DMPO)[58], which was also validated using high-resolution mass spectrometry (HRMS).

Theoretical studies

To reveal more mechanistic insights, the transfer methylation between **R1** and **1a** was computed using density functional theory (DFT) (Fig. 5 and see Supplementary Information, Section 5).

Upon the excitation and intersystem crossing (ISC) to the triplet ^{3}**R1**, the reaction starts with an intramolecular hydrogen atom transfer (HAT) between the α-aminomethyl group to the quinoline N atom of **R1** through ^{3}**TS1** (Fig. 5A). This HAT gives rise to the intermediate ^{3}**Int1** with spin centres localising on C10 of the DHPQ moiety and α-aminomethyl radical, respectively (Fig. 5B). Subsequently, ^{3}**Int1** evolves to the experimentally validated open-shell **Rc** via a proton-coupled electron transfer (PCET) process through ^{3}**TS2**[59,60]. During the

https://doi.org/10.1038/s41467-025-61857-0

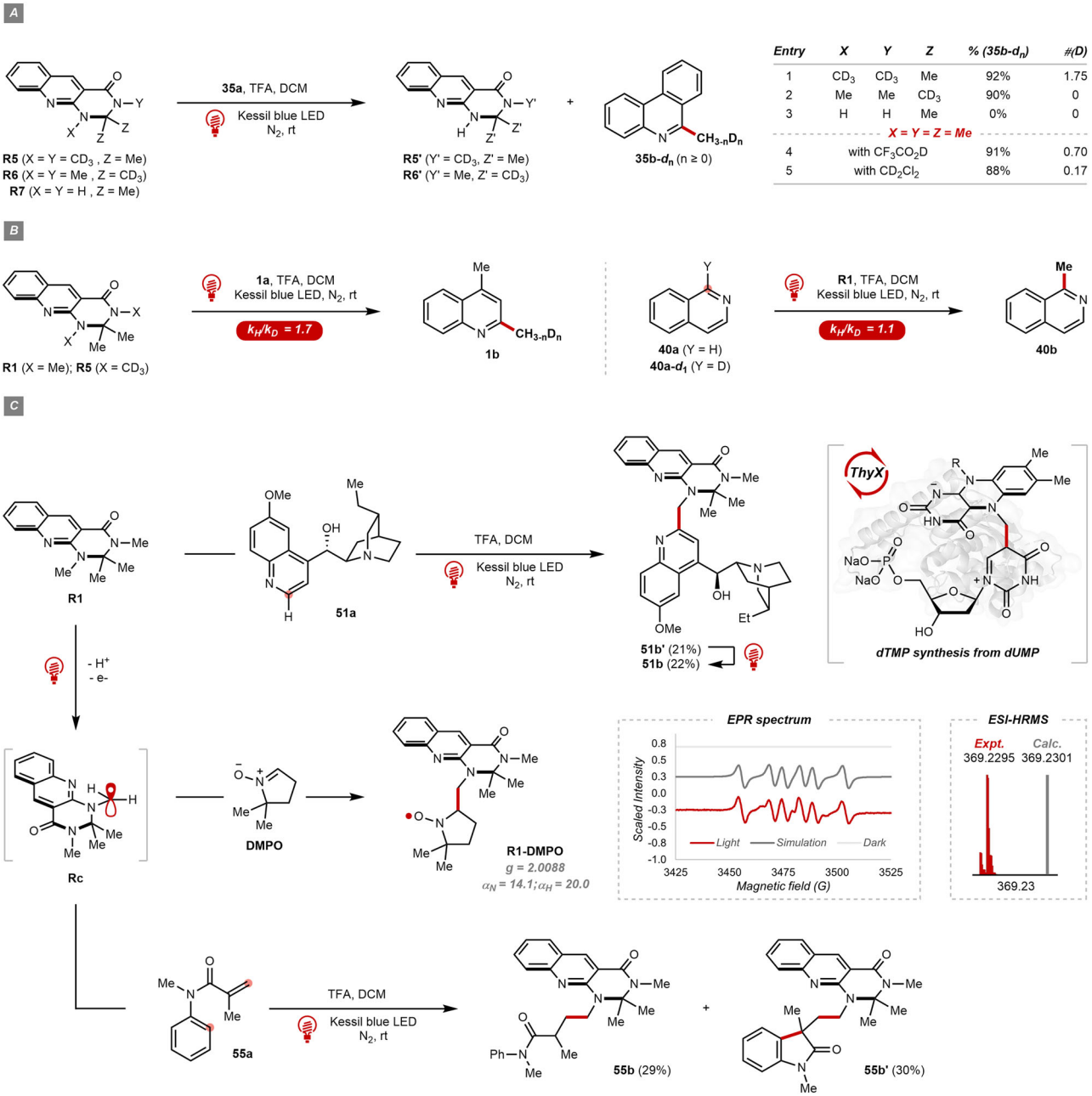

Fig. 4 | Mechanistic studies. See the Supplementary Information for detailed conditions. **A** Deuteration experiment. The deuterium degree is determined by NMR. TFA, trifluoroacetic acid. DCM, dichloromethane. LED, light-emitting diode. **B** Kinetic isotope effect (KIE) measurement. **C** Trapping of α-aminomethyl radical. DMPO, 5,5-dimethyl-1-pyrroline *N*-oxide. EPR, electron paramagnetic resonance. ESI-HRMS, electrospray ionisation high-resolution mass spectroscopy. dTMP, deoxythymidine monophosphate. dUMP, deoxyuridine monophosphate. Expt., experiment. Calc., calculation.

PCET, the proton is transferred from ^{3}**Int1** to the quinoline substrate (**1a**), accompanied by a gradual shift of spin densities from ^{3}**Int1** to the C4 of **1a** (Fig. 5B). The computed spin density and spin natural orbital evolutions for this process elucidate that as the forming N–H bond shrinks, the spin densities on the C10 position of ^{3}**Int1** diminish, while it emerges at the C4 of **1a** with almost identical amplitude. A reasonable barrier ($\Delta G^{\ddagger}$ = 13.1 kcal/mol) was found for such a PCET process, given that the sole single-proton transfer of ^{3}**Int1** would generate unstable charge-separated species with enhanced redox abilities. In contrast, the PCET process could circumvent the unfavourable charge separation by relocating the radical centre to **1a** and forming a hydrogen-bonded complex (^{3}**Int2_Rc**). For comparison, the energy barrier of direct Giese addition of ^{3}**Int1** with quinoline was found to be significantly higher than ^{3}**TS2**, further supporting this PCET process (Supplementary Fig. S11). Afterwards, the α-aminomethyl radical of **Rc** couples with quinoline radical at the C4 position through a nearly barrierless open-shell singlet transition state ^{oss}**TS3**, thus mechanistically diverging from the classic Minisci reaction and providing rationales to the uncommon regioselectivity in our case. Moreover, the calculated C2-methylation pathway proceeds at a higher barrier, and the $\Delta\Delta G^{\ddagger}$ = 0.50 kcal/mol matches our observed regioisomeric ratio.

After constructing the key C–C bond, another excitation and ISC event convert **Int3_C4** to its triplet counterpart, which further undergoes a similar HAT process via ^{3}**TS4**, relocating radical centres to two quinoline moieties in ^{3}**Int4_C4**. In the subsequent spin centre shift (SCS) via transition state ^{3}**TS5**, the N–C bond was homolysed, generating demethylated **R1'** and quinoline biradical intermediate ^{3}**1b** that will eventually be converted to the C4-methylated product (**1b**).

https://doi.org/10.1038/s41467-025-61857-0

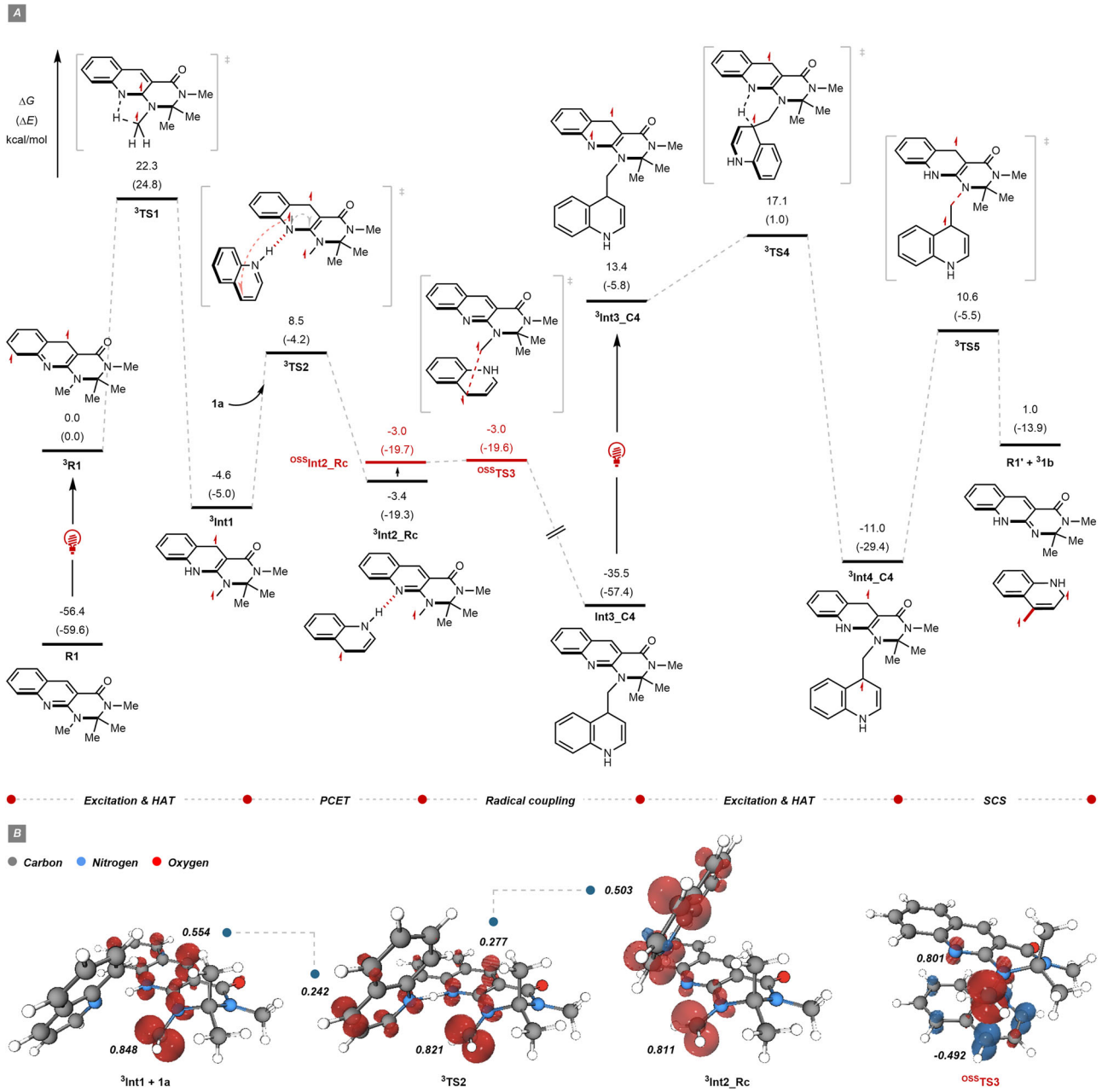

Fig. 5 | Density functional calculation of quinoline C(sp^2)–H methylation. **A** Calculated energy profiles for quinoline C(sp^2)–H methylation. Quantum chemical methods are employed at the B3LYP-D3(BJ)/SMD(DCM)/Def2TZVP//B3LYP-D3(BJ)/Def2SVP level of theory. TS, transition state. Int, intermediate. HAT, hydrogen atom transfer. PCET, proton-coupled electron transfer. SCS, spin-centre shift. **B** Mulliken spin densities for key species and transition states. The isovalue was set as 0.009.

Notably, the light intensity-regulated kinetics of **R1** are consistent with our proposed biphotonic regime (see Supplementary Information, Section 6.3)[61]. Overall, the self-sensitisation and group transfer mechanism of **R1** account for its unique reactivity and selectivity profile, which is worth further investigation.

Other synthetic applications with R1

Our transfer methylation method with **R1**, noted for its tolerance to various functional groups and aqueous environments, is well-suited for methylating complex and water-soluble molecules. Along this line, our strategy has been successfully applied to the water-soluble fibroblast activation protein inhibitor (FAPI) molecule (**56a**), enabling the efficient C(sp^2)–H methylation in mixed H_2O/DMSO solvent and the subsequent radiolabelling to assess the pharmacokinetic properties of the methylquinoline-based radiopharmaceuticals for tumour visualisation (Fig. 6A).

Other than heteroarenes, trisubstituted alkene, isocyanide and sulfone can be methylated under similar conditions (**57b**, **35b** and **37b**, Fig. 6B). In light of the halogen-atom transfer (XAT) modulated by α-aminoalkyl radicals, as pioneered by Leonori and Juliá for photocatalytic alkylation[44,45], we repurposed **R1** for other alkylative transformations with organohalides (Fig. 6C). DFT calculation predicted a favourable XAT process between our **Rc** and a selected bromide through a polarised transition state with considerable charge-transfer characters ($\delta^{TS} = 0.26$). Such a polar effect drove the homolytic cleavage of different C(sp^3)–Br bonds, leading to proto- (**60b**) and deuterodehalogenation (**61b**) products in the presence of a thiol organocatalyst (**R8**). Moreover, the benzyl radical could also be

https://doi.org/10.1038/s41467-025-61857-0

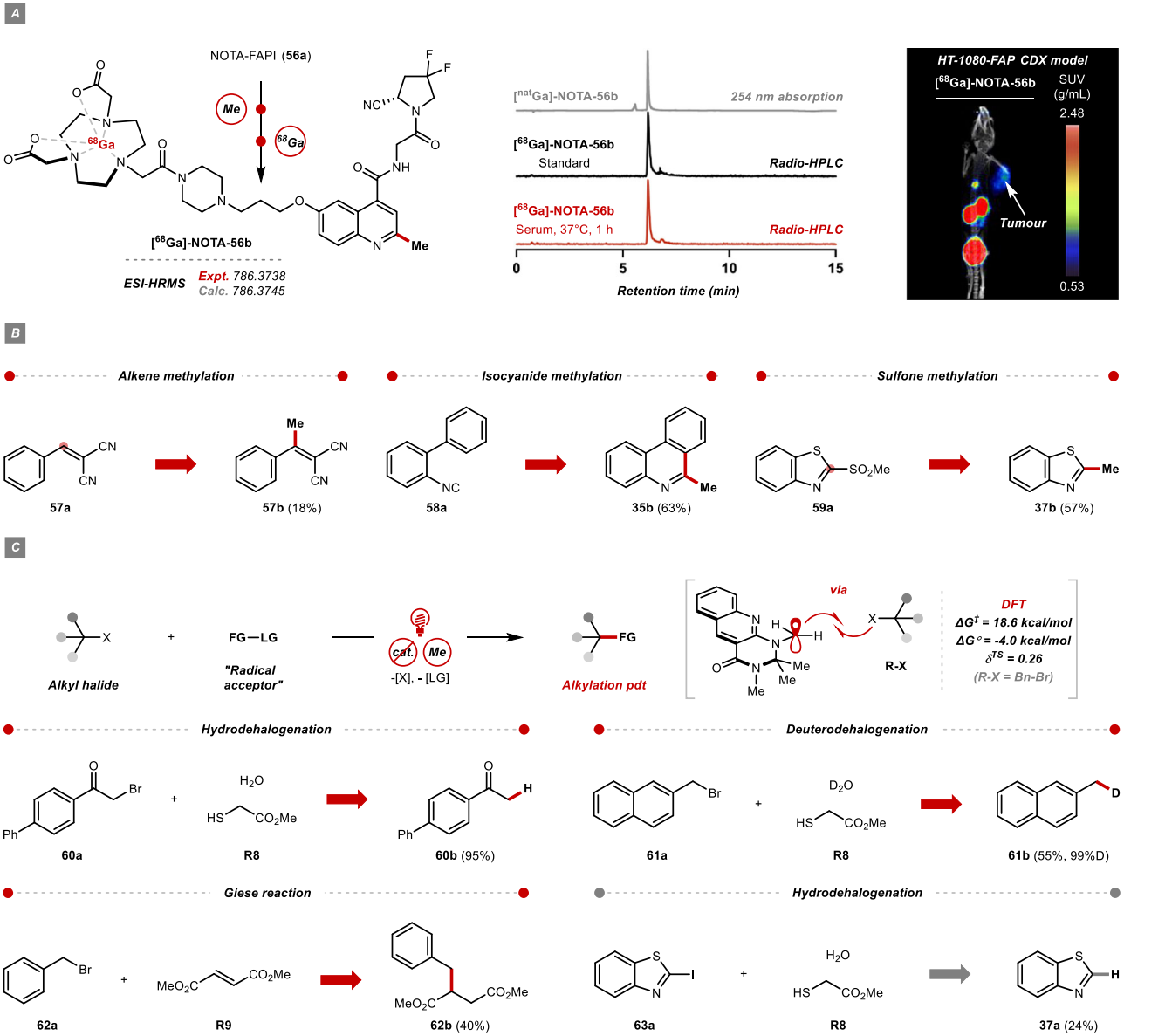

Fig. 6 | Other synthetic applications with R1. See the Supplementary Information for detailed conditions. **A** Pharmacokinetics studies of the methylated FAPI molecule. NOTA,1,4,7-triazacyclononane-1,4,7-triacetic acid. FAPI, fibroblast activation protein inhibitor. ESI-HRMS, electrospray ionisation high-resolution mass spectroscopy. HPLC, high-performance liquid chromatography. CDX, cell line-derived xenograft. SUV, standardised uptake value. Expt., experiment. Calc., calculation. **B** Methylation of alkene, isocyanide and sulfone. Yields are unoptimised. General conditions: radical acceptor (1.0 equiv), **R1** (1.5 equiv), TFA (3.0 equiv), DCM (0.050 M), Kessil lamp (427 nm). **C** XAT-mediated radical alkylation and arylation. Quantum chemical methods are employed at the B3LYP-D3(BJ)/SMD(DCM)/Def2TZVP//B3LYP-D3(BJ)/Def2SVP level of theory. XAT, halogen-atom transfer. FG, functional group. LG, leaving group. Pdt, product. R-X, alkyl halide. DFT, density functional theory. Bn, benzyl.

intercepted by dimethyl fumarate (**R9**), delivering the hydrobenzylation product in a moderate yield (**62b**). Lastly, reductive dehalogenation of aryl iodide was also possible (**37a**).

Discussion

Minisci-type methylation with (hydroxy)methyl radical has been known and extensively studied for over 50 years; however, a general laboratory method offering balanced reactivity and selectivity remained underdeveloped. In this contribution, we attempted to solve some facets of this problem with a biomimetic transfer methylating reagent (**R1**) that can generate a "bulky methyl" radical after direct excitation. While mechanistically related to the rSAM MT, our tailor-made **R1** can methylate a much broader range of substrates without photocatalysts and highly excessive radical precursors, thus equipping synthetic practitioners with a robust toolbox to access diverse methylated chemical entities. Comprehensive experimental and computational studies detailed the intermediacy of an α-aminomethylene radical. The conjugated heteroaromatic framework of such a radical was found instrumental for an efficient methyl group transfer, which also steered the non-classic C4–H selectivity of free quinoline, therefore complementing the current mainstay of methylation methodology. Moreover, the capability of **R1** to perform methylation on intricate molecules considerably decreases the synthetic workload, which could streamline the diversification of drug leads and, in turn, enhance the exploration of novel small-molecule therapeutics and chemical probes based on the "magic methyl" effect. Our ongoing research continues to delve deeper into the mechanisms of **R1** and its future iterations with the goal of expanding

the chemical space and synthetic reach of DHPQ reagents. We believe this work can provide some food for thought in addressing hitherto unsolved chemical challenges with bioinspiration and help demystify some related bioprocesses that remained poorly understood or unprecedented.

Methods

In a N_2-filled glovebox, to a 10 mL oven-dried Pyrex microwave tube equipped with a Teflon septum and a magnetic stir bar was added heteroarene (0.20 mmol, 1.0 equiv), **R1** (76.5 mg, 0.30 mmol, 1.5 equiv), TFA (45.9 µL, 68.4 mg, 0.60 mmol, 3.0 equiv) and DCM (0.050 M). The reaction tube was capped by the crimp seal with PTFE septum, removed from the glovebox and stirred at room temperature under the Kessil blue LED irradiation (λ = 427 nm, 45 W, 100% intensity). Upon consumption of the limiting reagent, as monitored by GC-MS or LC-MS, it was quenched by saturated $NaHCO_3$ solution and extracted by EtOAc three times. The combined organic layers were dried over Na_2SO_4 and concentrated under a vacuum to afford the crude product. The crude was purified by column chromatography over silica gel to furnish the desired product.

Reporting summary

Further information on research design is available in the Nature Portfolio Reporting Summary linked to this article.

Data availability

The X-ray crystallographic coordinates for structures of **R1** reported in this study have been deposited at the Cambridge Crystallographic Data Centre (CCDC), under deposition numbers 2389629. These data can be obtained free of charge from The Cambridge Crystallographic Data Centre via www.ccdc.cam.ac.uk/data_request/cif. All data generated in this study are available from the lead contact upon request. Source data are provided in this paper.

References

1. Aynetdinova, D. et al. Installing the "magic methyl" – C–H methylation in synthesis. *Chem. Soc. Rev.* **50**, 5517–5563 (2021).
2. Huang, J., Chen, Z. & Wu, J. Recent progress in methyl-radical-mediated methylation or demethylation reactions. *ACS Catal.* **11**, 10713–10732 (2021).
3. Li, Q.-Y., He, Y., Lin, Y.-M. & Gong, L. Photo-induced C–H methylation reactions. *Chem. Eur. J.* **29**, e202302542 (2023).
4. Liao, F. et al. Demystifying the recent photochemical and electrochemical tricks on installing the magic methyl group: A comprehensive overview. *Green. Chem.* **26**, 8161–8203 (2024).
5. Zhang, Z., Mahanta, N., Hudson, G. A., Mitchell, D. A. & van der Donk, W. A. Mechanism of a Class C radical *S*-adenosyl-L-methionine thiazole methyl transferase. *J. Am. Chem. Soc.* **139**, 18623–18631 (2017).
6. Mahanta, N., Zhang, Z., Hudson, G. A., van der Donk, W. A. & Mitchell, D. A. Reconstitution and substrate specificity of the radical *S*-adenosyl-methionine thiazole *C*-methyltransferase in thiomuracin biosynthesis. *J. Am. Chem. Soc.* **139**, 4310–4313 (2017).
7. Jones, P. A. & Takai, D. The role of DNA methylation in mammalian epigenetics. *Science* **293**, 1068–1070 (2001).
8. Barreiro, E. J., Kümmerle, A. E. & Fraga, C. A. M. The methylation effect in medicinal chemistry. *Chem. Rev.* **111**, 5215–5246 (2011).
9. Schönherr, H. & Cernak, T. Profound methyl effects in drug discovery and a call for new C–H methylation reactions. *Angew. Chem. Int. Ed.* **52**, 12256–12267 (2013).
10. Gui, J. et al. Methylation of heteroarenes inspired by radical SAM methyl transferase. *J. Am. Chem. Soc.* **136**, 4853–4856 (2014).
11. Minisci, F., Galli, R., Malatesta, V. & Caronna, T. Nucleophilic character of alkyl radicals—II: Selective alkylation of pyridine, quinoline and acridine by hydroperoxides and oxaziranes. *Tetrahedron* **26**, 4083–4091 (1970).
12. Jin, J. & MacMillan, D. W. C. Alcohols as alkylating agents in heteroarene C–H functionalization. *Nature* **525**, 87–90 (2015).
13. Liu, W., Yang, X., Zhou, Z.-Z. & Li, C.-J. Simple and clean photo-induced methylation of heteroarenes with MeOH. *Chem* **2**, 688–702 (2017).
14. Chang, L., An, Q., Duan, L., Feng, K. & Zuo, Z. Alkoxy radicals see the light: New paradigms of photochemical synthesis. *Chem. Rev.* **122**, 2429–2486 (2021).
15. An, Q. et al. Identification of alkoxy radicals as hydrogen atom transfer agents in Ce-catalyzed C–H functionalization. *J. Am. Chem. Soc.* **145**, 359–376 (2023).
16. Ang, H. T., Miao, Y., Ravelli, D. & Wu, J. Pyridine *N*-oxides as hydrogen atom transfer reagents for site-selective photoinduced C(sp^3)–H functionalization. *Nat. Synth.* **3**, 568–575 (2024).
17. Hu, A., Guo, J.-J., Pan, H. & Zuo, Z. Selective functionalization of methane, ethane, and higher alkanes by cerium photocatalysis. *Science* **361**, 668–672 (2018).
18. Yang, Q. et al. Photocatalytic C–H activation and the subtle role of chlorine radical complexation in reactivity. *Science* **372**, 847–852 (2021).
19. Yang, Q. et al. Mechanistic investigation of the Ce(III) chloride photoredox catalysis system: Understanding the role of alcohols as additives. *J. Am. Chem. Soc.* **147**, 2061–2076 (2025).
20. Duan, L., Lin, Y., An, Q. & Zuo, Z. Synergistic LMCT and Ni catalysis for methylative cross-coupling using *tert*-butanol: Modulating radical pathways via selective bond homolysis. *J. Am. Chem. Soc.* **147**, 14785–14796 (2025).
21. Studer, A. A "Renaissance" in radical trifluoromethylation. *Angew. Chem. Int. Ed.* **51**, 8950–8958 (2012).
22. Garza-Sanchez, R. A., Patra, T., Tlahuext-Aca, A., Strieth-Kalthoff, F. & Glorius, F. DMSO as a switchable alkylating agent in heteroarene C–H functionalization. *Chem. Eur. J.* **24**, 10064–10068 (2018).
23. Kariofillis, S. K., Shields, B. J., Tekle-Smith, M. A., Zacuto, M. J. & Doyle, A. G. Nickel/photoredox-catalyzed methylation of (hetero) aryl chlorides using trimethyl orthoformate as a methyl radical source. *J. Am. Chem. Soc.* **142**, 7683–7689 (2020).
24. McCallum, T., Pitre, S. P., Morin, M., Scaiano, J. C. & Barriault, L. The photochemical alkylation and reduction of heteroarenes. *Chem. Sci.* **8**, 7412–7418 (2017).
25. Laudadio, G. et al. Noël, T. C(sp^3)–H functionalizations of light hydrocarbons using decatungstate photocatalysis in flow. *Science* **369**, 92–96 (2020).
26. Pulcinella, A. et al. C1-4 alkylation of aryl bromides with light alkanes enabled by metallaphotocatalysis in flow. *Angew. Chem. Int. Ed.* **64**, e202413846 (2024).
27. Zhang, Y., Feng, J. & Li, C.-J. Palladium-catalyzed methylation of aryl C–H bond by using peroxides. *J. Am. Chem. Soc.* **130**, 2900–2901 (2008).
28. Dirocco, D. A. et al. Late-stage functionalization of biologically active heterocycles through photoredox catalysis. *Angew. Chem. Int. Ed.* **53**, 4802–4806 (2014).
29. Vasilopoulos, A., Krska, S. W. & Stahl, S. S. C(sp^3)–H methylation enabled by peroxide photosensitization and Ni-mediated radical coupling. *Science* **372**, 398–403 (2021).
30. Djossou, J. et al. Rapid methylation of aryl bromides using air-stable DABCO-bis (trimethylaluminum) via nickel metallaphotoredox catalysis. *Angew. Chem. Int. Ed.* e202508710 https://doi.org/10.1002/anie.202508710 (2025).
31. Josephitis, C. M., Nguyen, H. M. H. & McNally, A. Late-stage C–H functionalization of azines. *Chem. Rev.* **123**, 7655–7691 (2023).
32. O'Hara, F., Blackmond, D. G. & Baran, P. S. Radical-based regioselective C–H functionalization of electron-deficient heteroarenes: Scope, tunability, and predictability. *J. Am. Chem. Soc.* **135**, 12122–12134 (2013).

33. Choi, J., Laudadio, G., Godineau, E. & Baran, P. S. Practical and regioselective synthesis of C-4-alkylated pyridines. *J. Am. Chem. Soc.* **143**, 11927–11933 (2021).
34. Cao, H., Cheng, Q. & Studer, A. Radical and ionic *meta*-C–H functionalization of pyridines, quinolines, and isoquinolines. *Science* **378**, 779–785 (2022).
35. Kim, M., Koo, Y. & Hong, S. *N*-Functionalized pyridinium salts: A new chapter for site-selective pyridine C–H functionalization via radical-based processes under visible light irradiation. *Acc. Chem. Res.* **55**, 3043–3056 (2022).
36. Shi, Q., Huang, X., Yang, R. & Liu, W. H. Unified ionic and radical C-4 alkylation and arylation of pyridines. *Chem. Sci.* **15**, 12442–12450 (2024).
37. Xu, P. & Studer, A. Skeletal editing through cycloaddition and subsequent cycloreversion reactions. *Acc. Chem. Res.* **58**, 647–658 (2025).
38. Le Saux, E., Georgiou, E., Dmitriev, I. A., Hartley, W. C. & Melchiorre, P. Photochemical organocatalytic functionalization of pyridines via pyridinyl radicals. *J. Am. Chem. Soc.* **145**, 47–52 (2022).
39. Prier, C. K., Rankic, D. A. & MacMillan, D. W. C. Visible light photoredox catalysis with transition metal complexes: Applications in organic synthesis. *Chem. Rev.* **113**, 5322–5363 (2013).
40. Shaw, M. H., Twilton, J. & MacMillan, D. W. C. Photoredox catalysis in organic chemistry. *J. Org. Chem.* **81**, 6898–6926 (2016).
41. Sato, Y. et al. Generation of alkyl radical through direct excitation of boracene-based alkylborate. *J. Am. Chem. Soc.* **142**, 9938–9943 (2020).
42. Sumida, Y. & Ohmiya, H. Direct excitation strategy for radical generation in organic synthesis. *Chem. Soc. Rev.* **50**, 6320–6332 (2021).
43. Li, J., Zhang, D., Tan, L. & Li, C.-J. Direct excitation strategy for deacylative couplings of ketones. *Angew. Chem. Int. Ed.* **63**, e202410363 (2024).
44. Constantin, T. et al. Aminoalkyl radicals as halogen-atom transfer agents for activation of alkyl and aryl halides. *Science* **367**, 1021–1026 (2020).
45. Juliá, F., Constantin, T. & Leonori, D. Applications of halogen-atom transfer (XAT) for the generation of carbon radicals in synthetic photochemistry and photocatalysis. *Chem. Rev.* **122**, 2292–2352 (2022).
46. Pitzer, L., Schäfers, F. & Glorius, F. Rapid assessment of the reaction-condition-based sensitivity of chemical transformations. *Angew. Chem. Int. Ed.* **58**, 8572–8576 (2019).
47. Ruffoni, A., Hampton, C., Simonetti, M. & Leonori, D. Photoexcited nitroarenes for the oxidative cleavage of alkenes. *Nature* **610**, 81–86 (2022).
48. Wise, D. E. et al. Photoinduced oxygen transfer using nitroarenes for the anaerobic cleavage of alkenes. *J. Am. Chem. Soc.* **144**, 15437–15442 (2022).
49. Gkizis, P. L., Triandafillidi, I. & Kokotos, C. G. Nitroarenes: The rediscovery of their photochemistry opens new avenues in organic synthesis. *Chem* **9**, 3401–3414 (2023).
50. Woo, J. et al. Scaffold hopping by net photochemical carbon deletion of azaarenes. *Science* **376**, 527–532 (2022).
51. Jurczyk, J. et al. Single-atom logic for heterocycle editing. *Nat. Synth.* **1**, 352–364 (2022).
52. Terunuma, T., Kawauchi, G. & Hayashi, Y. Organocatalyst mediated pot-economical total synthesis of (−)-quinine and its derivatives. *Asian J. Org. Chem.* **12**, e202300256 (2023).
53. Kim, L., Lee, W. & Hong, S. Insight into C4 selectivity in the light-driven C–H fluoroalkylation of pyridines and quinolines. *Angew. Chem. Int. Ed.* **63**, e202410408 (2024).
54. Proctor, R. S. J., Davis, H. J. & Phipps, R. J. Catalytic enantioselective Minisci-type addition to heteroarenes. *Science* **360**, 419–422 (2018).
55. Proctor, R. S. J. & Phipps, R. J. Recent advances in Minisci-type reactions. *Angew. Chem. Int. Ed.* **58**, 13666–13699 (2019).
56. Ermanis, K. et al. A computational and experimental investigation of the origin of selectivity in the chiral phosphoric acid catalyzed enantioselective Minisci reaction. *J. Am. Chem. Soc.* **142**, 21091–21101 (2020).
57. Bou-Nader, C. et al. An enzymatic activation of formaldehyde for nucleotide methylation. *Nat. Commun.* **12**, 4542 (2021).
58. Leifert, D. & Studer, A. The persistent radical effect in organic synthesis. *Angew. Chem. Int. Ed.* **59**, 74–108 (2020).
59. Shi, Q. et al. Diradical generation via relayed proton-coupled electron transfer. *J. Am. Chem. Soc.* **144**, 3137–3145 (2022).
60. Wang, Y., Chen, W., Lai, Y. & Duan, A. Activation model and origins of selectivity for chiral phosphoric acid catalyzed diradical reactions. *J. Am. Chem. Soc.* **145**, 23527–23532 (2023).
61. Glaser, F., Kerzig, C. & Wenger, O. S. Multi-photon excitation in photoredox catalysis: Concepts, applications, methods. *Angew. Chem. Int. Ed.* **59**, 10266–10284 (2020).

Acknowledgements

The authors are grateful for the financial support, including the University Development Fund-Research Start-up Fund (UDF01003552) from the Chinese University of Hong Kong, Shenzhen, fund from the National Natural Science Foundation of China (NSFC22401240) and Guangdong Basic Research Centre of Excellence for Aggregate Science, to J.L.; the NSERC, FQRNT, CFI, and Canada Research Chairs funds to C.-J.L.; fund from the Ministry of Science and Technology of the People's Republic of China (Grant No. 2021YFA1601400) to Z.L. and fund from the National Natural Science Foundation of China (NSFC22203034) to Z.Z. J.L. is indebted to the IUPAC-Solvay International Awards for Young Chemists and the IUPAC-Zhejiang NHU International Award for Advancements in Green Chemistry. Z.Y., thanks for the Undergraduate Research Award. J.L. would like to thank the generous donation of chemicals and sharing of equipment from several laboratories in the School of Science and Engineering (SSE), CUHK-Shenzhen, including those supervised by Professor Henry N. C. Wong/Xiaoshui Peng/Jianfang Cui, Professor Ben Zhong Tang/Zheng Zhao/Zijie Qiu/Jianquan Zhang, Professor Zhihai Ke and Professor Zhongxin Chen. J.L. would also like to acknowledge the contribution of staff at the Material Characterisation and Preparation Centre (MCPC) in the SSE, CUHK-Shenzhen (Ms. Guimiao Liu and Mr. Yang Kong) and the McGill Chemistry Characterisation Facility (Dr. Kirill Levin and Dr. Hatem Titi) for the compound characterisation in this work. Besides, J.L. thanks Dr. Chia-Yu Huang (University of North Carolina at Chapel Hill) for discussing the initial findings of this work and Dr. Bingqing Liu (University of Illinois, Chicago) for discussing the TCSPC. Lastly, J.L. thanks Dr. Zihang Qiu (Dalian University of Technology) and Dr. Chen-Chen Li (Eurofins Canada) for polishing this manuscript.

Author contributions

J.L. secured the funding, supervised the projects, conceived and designed the reactions, completed the preliminary optimisation and substrate scope, conducted the mechanistic studies, wrote the manuscript, and prepared the Supplementary Information. C.-J.L. secured the funding and supervised the projects. Z.L. secured the funding and supervised the projects. Z.Z. secured the funding and performed the calculation. Z.H. prepared the non-commercial substrates. Z.Y. prepared the methylating reagent and the non-commercial substrates. L.T. performed the EPR, crystallisation and UV-mediated methylation reactions. W.L. finished the radiolabelling and pharmacokinetic experiments. D.Z. finished the HTE and control experiments, explored the substrate scope, and prepared the Supplementary Information. All authors approved the final version of the manuscript.

Competing interests

The author declares no competing interests.

Inclusion & ethical statement

All animal experiments were performed according to the Animal Protection Guidelines of Peking University, China. All animal care and experimental procedures were performed by following the animal protocols (CCME-LiuZB-2) approved by the ethics committee of Peking University. According to the protocols, the tumour volumes are all lower than 1,500 mm^3 in all animal experiments.

Additional information

Supplementary information The online version contains supplementary material available at https://doi.org/10.1038/s41467-025-61857-0.

Correspondence and requests for materials should be addressed to Zhihan Zhang, Zhibo Liu, Chao-Jun Li or Jianbin Li.

Peer review information *Nature Communications* thanks Yuto Sumida, qingmin Wang and the other anonymous reviewer(s) for their contribution to the peer review of this work. A peer review file is available.